$L_g = 100$ nm T-shaped gate AlGaN/GaN HEMTs on Si substrates with non-planar source/drain regrowth of highly-doped n^+-GaN layer by MOCVD*

Huang Jie(黄 杰)[a)†], Li Ming(黎 明)[b)‡], Tang Chak-Wah(邓泽华)[b)], and Lau Kei-May(刘纪美)[b)]

[a)] College of Engineering and Technology, Southwest University, Chongqing 400715, China

[b)] Department of Electronic and Computer Engineering, Hong Kong University of Science and Technology, Hong Kong, China

(Received 6 March 2014; revised manuscript received 31 July 2014; published online 10 October 2014)

High-performance AlGaN/GaN high electron mobility transistors (HEMTs) grown on silicon substrates by metal–organic chemical-vapor deposition (MOCVD) with a selective non-planar n-type GaN source/drain (S/D) regrowth are reported. A device exhibited a non-alloyed Ohmic contact resistance of 0.209 Ω·mm and a comprehensive transconductance (g_m) of 247 mS/mm. The current gain cutoff frequency f_T and maximum oscillation frequency f_{MAX} of 100-nm HEMT with S/D regrowth were measured to be 65 GHz and 69 GHz. Compared with those of the standard GaN HEMT on silicon substrate, the f_T and f_{MAX} is 50% and 52% higher, respectively.

Keywords: GaN, HEMTs, S/D (S/D) regrowth, MOCVD

PACS: 81.05.Ea **DOI:** 10.1088/1674-1056/23/12/128102

1. Introduction

AlGaN/GaN-based high-electron-mobility transistors (HEMTs) on Si substrate have attracted a lot of interest in the semiconductor community because of their high breakdown voltage, high electron saturation velocity, and the integration with advanced Si-based complementary metal oxide semiconductor (CMOS) technology. Owing to these properties, GaN-based HEMTs are particularly attractive for the applications of digital-analog (DA) and analog-digital (AD) converters and radio frequency (RF) power amplifiers.

Even then, the power efficiency of AlGaN/GaN HEMTs is still limited by high ON-state resistance resistances, of which high source and drain Ohmic contact resistances are a main contribution. For decades, researchers have tried to obtain low ON-state resistance by utilizing several techniques, such as ion-implantation, surface treatment, and selective area growth (SAG). The use of ion-implantation is widespread in CMOS self-aligned technology. Numerous studies about GaN Ohmic contacts based on ion-implantation technology have been reported. Satoh *et al*. demonstrated an ultra-low resistive Ohmic contact of 1.2×10^{-7} Ω·cm^2.[1] However, the high annealing temperatures (1100 °C–1500 °C) limit the use of ion implantation for GaN material during the device fabrication procedure due to the fact that the high temperature process is generally associated with activating implanted dopants to substitutional sites.[2] The annealing temperature is already higher than the expital material growth temperature of MOCVD. Such high temperatures can cause a series of problems, such as GaN film dissociation, Si dopant diffusion and surface degradation dissociation.

SAG of highly doped n-type GaN is another attractive technique among various "S/D" engineering methods, and furthermore, most methods of SAG are generally based on MBE technology.[3–7] As shown in Fig. 1, GaN HEMT based on SAG technology by MOCVD presents some significant advantages over that based on ion implantation. Compared with the ion implantation, SAG gives GaN HEMT the most important advantage of providing heavily doped S/D by MOCVD with less crystal damage or post-annealing, which leads to a reduction of parasitic elements and an enhancement of tunneling transport of electrons. It is particularly important for scaled devices.[8,9] Moreover, due to the high stress channel and damage-free nature, the off-state breakdown voltage of GaN-based HEMT with the SAG process can be increased dramatically.[10] A high breakdown voltage is crucial for high-power GaN devices.

Since the SAG of n^+-GaN is quite critical to reducing R_{ON} of GaN HEMTs, in this work, highly-doped n^+-GaN was selectively regrown in the S/D to lower the contact resistance. Finally, both the DC and RF performance of GaN HEMT based on SAG technology were measured and compared with standard AlGaN/GaN HEMTs.

*Project supported by the Young Scientists Fund of the National Natural Science Foundation of China (Grant No. 61401373), the Fundamental Research Funds for Central Universities, China (Grant No. XDJK2013B004), and the Research Fund for the Doctoral Program of Southwest University, China (Grant No. SWU111030).

†Corresponding author. E-mail: jiehuang@swu.edu.cn

‡Corresponding author. E-mail: eeliming@sina.com

© 2014 Chinese Physical Society and IOP Publishing Ltd

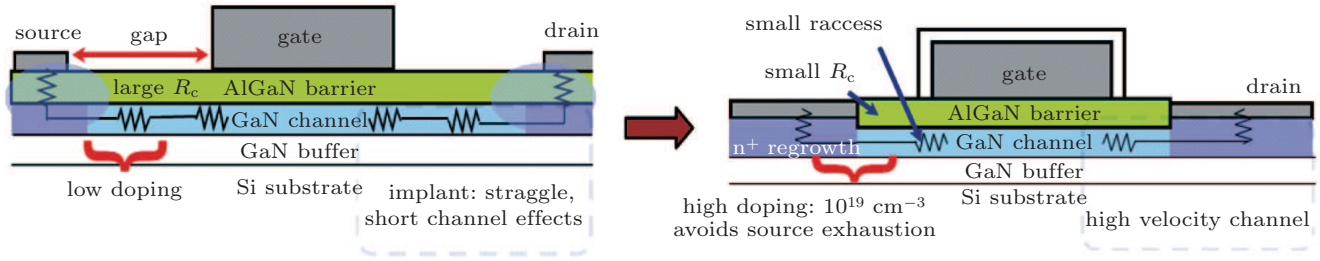


Fig. 1. (color online) A schematic diagram of the GaN HEMT "SAG" process by MOCVD.

2. Experiment

The AlGaN/GaN HEMT expital material was grown on 2-inch (1 inch = 2.54 cm) n-type silicon (111) substrates by the MOCVD system. The entire expital layer structure of the AlGaN/GaN HEMT on Si (111) substrates is shown in Fig. 2.

A 40-nm-thick AlN nucleation layer was deposited at 1150 °C, followed by the SiN_x mask layer growth at 1160 °C. This *in situ* mask did not cover the surface completely and served the purpose of enhancing the lateral growth of GaN with incomplete coverage. Then, a 0.8-μm-thick undoped GaN transition layer was grown uniformly on the exposed AlN nucleation layer with lateral overgrowth on the SiN_X mask layer at 1170 °C. Stacked AlGaN/AlN interlayers were grown on the GaN transition layer to further reduce the tensile stress, with the growth temperature being held at 950 °C for the AlN layer and 1150 °C for the AlGaN layer. Subsequently, a continuous 1.00-μm-thick GaN buffer (consisting of an 875-nm-thick un-doped portion on top of a 125-nm-thick Mg^{2+}-doped lower region) was grown at 1170 °C. Finally, the upper HEMT structure was grown, including a 1-nm AlN, and AlGaN with undoped and doped layers. The root mean square (RMS) value of surface roughness is 1.6 nm across a scanned area of 5 μm×5 μm. In Fig. 2, which demonstrates a smooth surface compared to our previous work.[11]

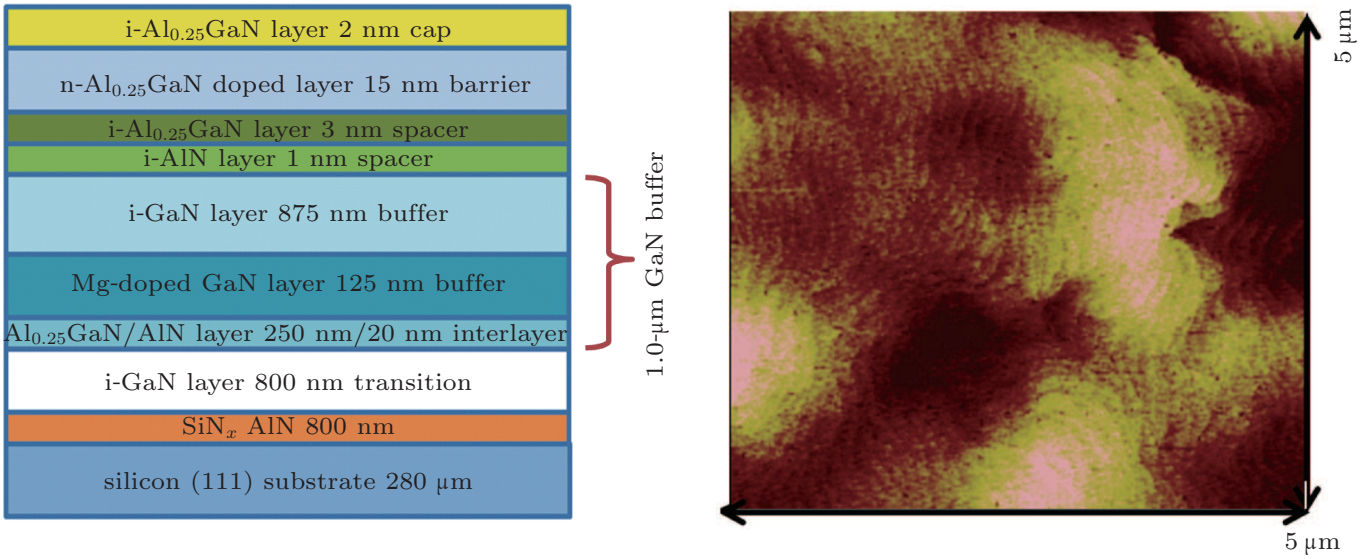
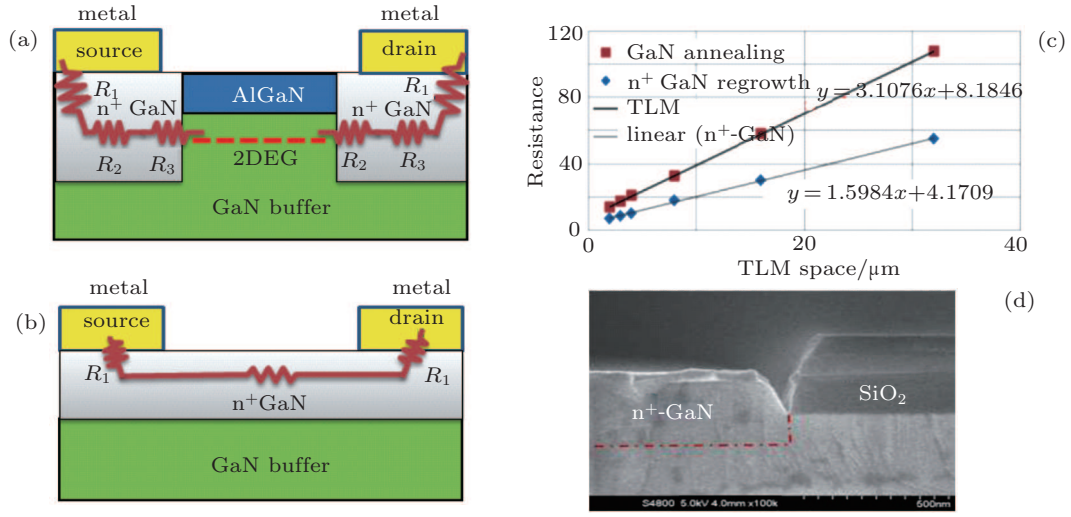


Fig. 2. (color online) Schematic plot of AlGaN/GaN HEMT structure on Si substrates and atomic force microscope (AFM) picture.

For the regrowth process, the S/D region was first etched down to the GaN channel with SiO_2 as the regrowth pattern mask. Then the sample was loaded into the MOCVD system. Selective regrowth of n^+GaN was performed at 1155 °C. Good selectivity was achieved. Figure 3(d) illustrates the cross-section schematics of GaN-based HEMTs with the regrown S/D process. The no-planer SAG process was found to be difficult to control the regrowth rate by MOCVD, and therefore the regrown S/D region is slightly higher than the normal one. Finally, the SiO_2 mask was removed by BOE subsequently. According to Hall measurement of planer n^+-GaN regrowth on samples without SiO_2 patterns, the Si doping concentration is estimated to be around 1×10^{19} cm^3. In addtion, to facilitate device comparison, a standard HEMT was also processed. The detailed process is the same as in our previous work;[12] the spacing of gate–source and gate–drain were both 1.5 μm.



(e) Patterns	n+ GaN regrowth	GaN annealing (850 ℃)
R_c/Ω·mm	0.209	0.409
r_c/Ω·cm^2	2.73×10^{-6}	5.40×10^{-6}
R_1, R_2, and R_3	(0.11), (0.043), and (0.056)	

Fig. 3. (color online) (a) Schematics of the MOCVD-regrown contact TLM pattern on HEMT heterostructure, (b) MOCVD-regrown n$^+$ GaN (control), (c) and (e) the TLM comparison, and (d) the SEM image of the regrowth cross section in the HEMT.

3. Experiment and discussion

Ohmic contact resistances (R_c) were measured using the transmission-line method (TLM) technique. As shown in Fig. 3(a), R_c can be divided into three components: R_1, resistance between the Ohmic metal and regrown n$^+$-GaN; R_2, resistance of the n$^+$-GaN access region; and R_3, resistance between regrown n$^+$-GaN and the two-dimension electron gas (2DEG) channel. To extract each component resistance, TLMs were made on the same wafer where the AlGaN barrier was etched away and the n$^+$-GaN was regrown, and the control TLMs can be referred to Fig. 3(b). It is assumed that the metal/n$^+$-GaN resistance R_1 is equal to the contact resistance extracted from the control TLMs. The R_c is determined to be 0.209 Ω·mm for the HEMT with SAG, and is lower than 0.409 Ω·mm for standard HEMT with 850-°C annealing temperature. The lower R_c indicates a high doping level in the regrown GaN S/D region.

Figures 4(a) and 4(b) illustrate the output and transfer characteristics of the standard 1-μm gate-length HEMT and the similar HEMT with the S/D regrowth process, and both show excellent pinch-off and saturation characteristics. The HEMT with SAG achieves a threshold voltage V_T of −2.4 V and a saturation current I_{Dsat} of 902 mA/mm at $V_{GS} = 1.5$ V, and peak trans-conductance G_m of 247 mS/mm at $V_{DS} = 6$ V, while standard HEMT shows V_T of −2.2 V, I_{Dsat} of 870 mA/mm at $V_{GS} = 1.5$ V, and peak G_m of 245 mS/mm at $V_{DS} = 6$ V. It is obviously noted that the on-state resistance R_{on} of the HEMT with SAG (2.22 Ω·mm) is almost half the resistance of the standard HEMT (3.96 Ω·mm) and that the corresponding measured Ohmic contact resistance R_c is similar to the two devices.

Figure 5(a) shows the measured gate leakage current of the HEMTs with and without SAG. The gate leakage current I_G of the standard HEMT and HEMT with SAG at a gate bias V_{GS} of −35 V is 0.02 mA/mm and 0.04 mA/mm, respectively. It is expected that the leakage current would be further-reduced by appropriate post-process treatments.

In addition, the "off-state" breakdown voltage V_{Br} of GaN-based HEMT with SAG can be increased dramatically to 120 V, in comparison with V_{Br} of 41 V of the standard HEMT, which can be found in Fig. 5(b). The gate-length L_g, gate-source space L_{gs}, gate–drain space L_{gd}, and gate-width W_g of the two HEMTs are both 1 μm, 1 μm, 2 μm, and 10 μm, respectively. It is noted that the damage-free SAG process seems to avoid the creation of defects in the doped region, thereby suppressing the drain leakage current and improving breakdown behavior.[10] So it is expected that the breakdown voltage will be further improved if SAG is combined with the other methods mentioned in Refs. [13]–[15].

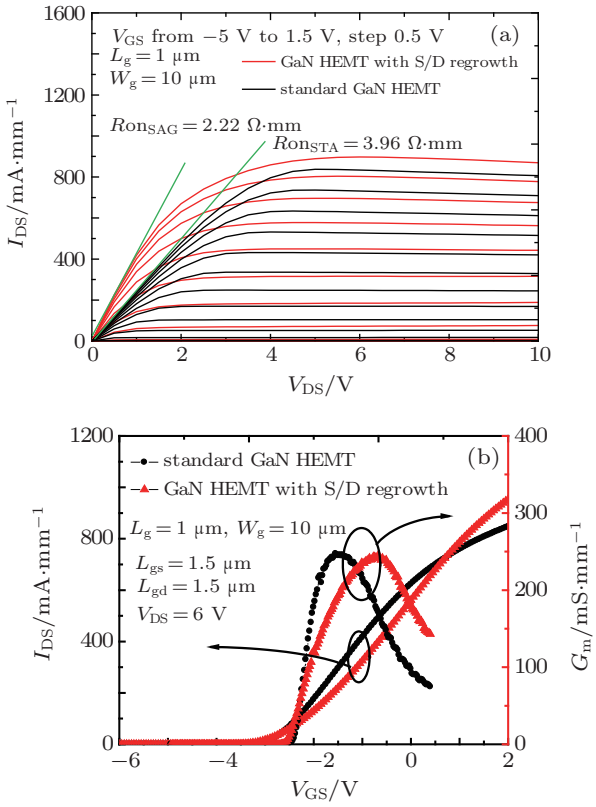


Fig. 4. (color online) (a) Typical *I*–*V* characteristics of a GaN HEMT (V_{GS} from −5 V to 1.5 V, step 0.5 V) and (b) transfer characteristics of GaN HEMT.

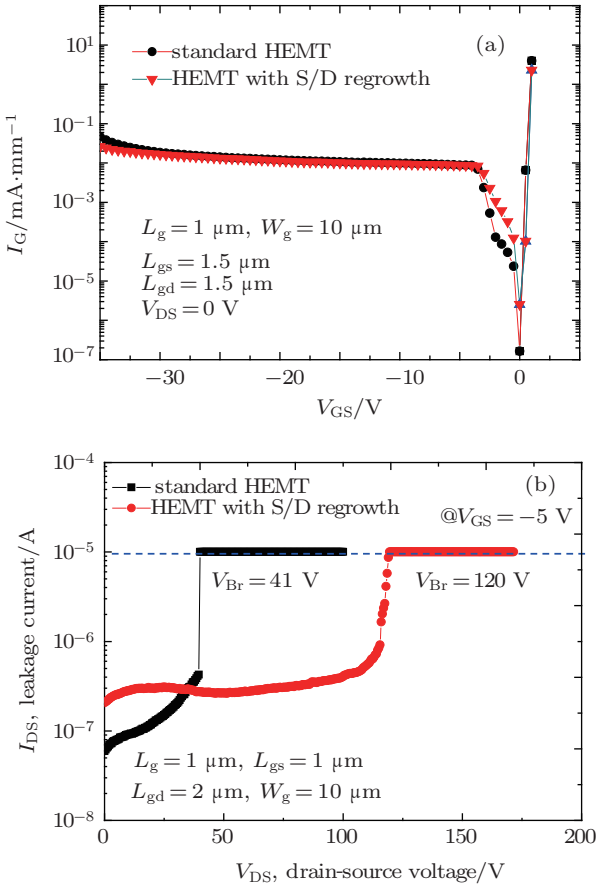


Fig. 5. (color online) (a) Measured gate leakage current as a function of gate bias, (b) the "off-state" breakdown voltage of GaN-based HEMT.

The comparison of RF characteristics between the standard HEMT and HEMT with SAG was also performed on 0.1 μm×100 μm GaN HEMTs by Cascade Microtech probes and an HP8722 network analyzer from 0.1 GHz to 39.1 GHz. As presented in Fig. 6, 100-nm gate length AlGaN/GaN HEMT with SAG exhibits an f_T of 65 GHz and an f_{max} of 69 GHz, while the standard HEMT shows an f_T of 31.3 GHz and an f_{max} of 22.3 GHz. Although the HEMT with SAG achieves a comparable extrinsic G_m to the standard HEMT, if almost double the current cutoff frequency f_T . Gate-to-Source capacitance C_{gs} and Gate-to-Drain capacitance C_{gd} were extracted from *S*-parameters at peak G_m gate bias voltage. The HEMT with SAG achieves a C_{gs} of 0.466 pF/mm and a C_{gd} of 0.031 pF/mm, much lower than that of the standard HEMT (C_{gs} of 0.786 pF/mm, C_{gd} of 0.052 pF/mm). The drastically reduced C_{gs} and C_{gd} result in a higher ratio of transconductance to gate capacitance, leading to the significant improvement of RF performances.

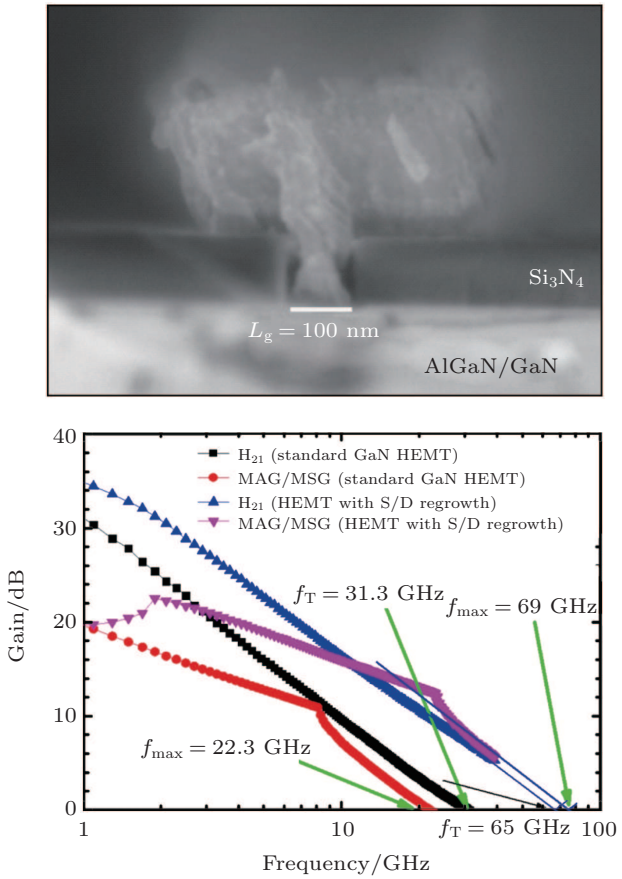


Fig. 6. (color online) SEM picture of 100-nm T-shaped gate and small signal RF characteristics of 0.1 μm×100 μm devices.

4. Conclusion

The incorporation of highly doped n^+-GaN S/D selective regrowth by MOCVD in AlGaN/GaN HEMTs on a Si substrate has been experimentally demonstrated. Significant improvement of device RF performance was observed. These re-

sults suggest the potential of using Si as substrates for the low-cost manufacture of high-performance power devices. To fully explore the benefits of selective S/D regrowth in III–V transistors, optimization of both material growth and device structure are carried out. The exceptional high frequency performance together with very low R_{on}, high G_m, and high breakdown voltage V_{Br} will make this device suitable for various applications such as high frequency PAs and robust low-noise amplifiers (LNAs).

References

[1] Nomoto K, Tajima T, Mishima T, Satoh M and Nakamura T 2007 *IEEE Electron Dev. Lett.* **28** 939

[2] Kambayashi H, Niiyama Y, Ootomo S, Nomura T, Iwami M, Satoh Y, Kato S and Yoshida S 2007 *IEEE Electron Dev. Lett.* **28** 1077

[3] Guo J, Guo W L and Cao Y 2012 *IEEE Electron Dev. Lett.* **33** 525

[4] Guo J, Cao Y, Lian C X, Zimmermann T, Li G W, Verma J, Gao X, Guo S P, Paul S, Mark W and Xing H L 2011 *Physica Status Solidi* **208** 1617

[5] Yue Y Z, Hu Z Y, Guo J and Rodriguez S 2012 *IEEE Electron Dev. Lett.* **33** 988

[6] Shinohara K, Corrion A, Regan D, Milosavljevic I, Brown D, Burnham S, Willadsen P J, Butler C, Schmitz A, Wheeler D, Fung A and Micovic M 2010 *IEEE International Electron Devices Meeting*, December 6–8, 2010, San Franciso, CA, p. 301.1

[7] Pang L, Zheng Z, Seo H C, Chapman P, Krein P, Lee J H, Kim K W and Kim K 2010 18*th Biennial University/Government/Industry Micro/Nano Symposium* (UGIM), June 28, 2010, West Lafayette, Indiana, p. 1

[8] Singisetti U, Wistey M A, Burek G J, Baraskar A K, Cagnon J, Thibeault B, Gossard A C, Stemmer S, Rodwell M J W, Kim E, Shin B, McIntyre P C and Lee Y J 2009 *IEEE IPRM*, May 10–14, 2009 Newport Beach, CA, p. 120

[9] Takenaka M, Takeda K, Hoshii T, Tanemura T, Sugiyama M, Nakano Y and Takagi S 2009 *IEEE IPRM*, May 10–14, 2009, Newport Beach, CA, p. 111

[10] Liang P, Chan S H, Patrick C, Ilesanmi A and Kim K 2010 *J. Election. Mater.* **39** 499

[11] Wang Y, Yu N S, Deng D M, Li M, Sun F, Lau K M 2010 *Sci. China: Phys. Mech. & Astron.* **53** 1578

[12] Wang Y, Yu N S, Li M, Lau K M 2011 *Chin. Phys. Lett.* **28** 057102

[13] Bahat-Treidel E, Hilt O, Brunner F, Wu J and Trankle G 2008 *IEEE Trans. Electron. Dev.* **55** 3354

[14] Yagi S, Shimizu M, Okumura H, Ohashi H, Yano Y and Akutsu N 2007 *J. Appl. Phys.* **46** 2309

[15] Song D, Liu J, Cheng Z, Tang W C, Lau K M and Chen K J 2007 *Proceedings of the* 19*th International Symposium on Power Semiconductor Devices & IC's*, May 27–31, 2007, Jeju, Island, p. 257